2018-2

by 2 2018

Submission date: 08-Aug-2021 01:22PM (UTC+0700)
Submission ID: 1628964369
File name: 2018_artikel_drm_jurnal_inter_Molecular_Cat_penulis_anggota.pdf (1.57M)
Word count: 7697
Character count: 37183

Molecular Catalysis 445 (2018) 52–60

Contents lists available at ScienceDirect

Molecular Catalysis

journal homepage: www.elsevier.com/locate/mcat

Research Paper

Novel preparation method of bimetallic Ni-In alloy catalysts supported on amorphous alumina for the highly selective hydrogenation of furfural

Rodiansono[a,*], Maria Dewi Astuti[a], Dwi Rasy Mujiyanti[a], Uripto Trisno Santoso[a], Shogo Shimazu[b,*]

[a] Department of Chemistry, Lambung Mangkurat University, Jl. A. Yani Km 36 Banjarbaru 70714, Indonesia
[b] Graduate School of Engineering, Chiba University, 1-33 Yayoi, Inage, Chiba, 263-8522, Japan

ARTICLE INFO

Article history:
Received 11 July 2017
Received in revised form 31 October 2017
Accepted 2 November 2017

Keywords:
Bimetallic Ni-In alloy catalyst
Selective hydrogenation
Biomass-derived furfural
Furfuryl alcohol

ABSTRACT

A novel preparation method for bimetallic nickel-indium alloy catalysts supported on amorphous alumina (Ni-In(x)/AA; x = Ni/In molar ratio) catalysts has been developed and evaluated for the highly selective hydrogenation of biomass-derived furfural. Ni-In(*x*)/AA catalysts were obtained via the hydrothermal treatment of Raney® nickel supported on aluminium hydroxide (R-Ni/AlOH) and an $InCl_2 \cdot H_2O$ solution in an ethanol/H_2O mixture at 423 K for 2 h, followed by reduction with H_2 at 573–873 K for 1.5 h. The formation of Ni-In alloy phases such as Ni_3In_2, Ni_3In, Ni_2In, and NiIn in Ni-In(*2.0*)/AA was clearly observed after reduction with H_2 at 873 K for 1.5 h. Ni-In(*2.0*)/AA contained a Ni_2In alloy as the major phase, which exhibited the best catalytic performance for the selective hydrogenation of furfural into furfuryl alcohol and was stable for at least five consecutive reaction runs.

1. Introduction

Biomass feedstock valorizations are currently being explored by using heterogeneous catalysts to produce bio-based platform chemicals, fuels, and various commodity products. Furfural (F) is one of the most promising biorefinery platform molecules because it can be transformed into a wide range of value-added derivative molecules, which can be used as plasticizers, solvents, agrochemicals, monomers in the production of resins (e.g., furfuryl alcohol (FA) and tetrahydrofurfuryl alcohol (THFA)) and gasoline blends (e.g., methyl furan (MF) or terminal diols (e.g., pentanediol (PD)) [1–3]. F could be produced effectively from C-5 sugars in hemicellulosic biomasses, such as xylan, arabinose and C-6 sugars in form of glucose or fructose via acidic hydrolysis [4–6].Autor name:

Interactions between metals in bimetallic catalysts can modify their surfaces, which can be beneficial for the conversion and upgrading of highly complex biomass fractions[7–9]. Copper-chromite was the first industrial bimetallic catalyst for the hydrogenation of F under harsh reaction conditions (473–573 K, 20–30 MPa) with maximum FA yields of ca. 70% [10]. In previously published studies, several bimetallic alloy transition metal catalysts (e.g., Ni-Sn [11–13], Ni-Fe [14,15], Ni-In [16] Pd-Cu [17], and Pt-Zn [18]) have shown superior performance for the selective hydrogenation of F compared with their single metal counterpart. Delbecq et al. have suggested that an increase in the charge density of Pt metals by the addition of hyperelectronic metals or the formation of a metal alloy could enhance the affinity towards the C=O bond rather than towards the C=C bond to form unsaturated alcohols in the hydrogenation of α,β-unsaturated aldehydes [19,20]. Moreover, unlike tin alloyed with Pt, the utilization of Ni-Sn alloy-based catalysts for the selective hydrogenation of unsaturated carbonyl compounds has been rarely investigated to date [21].

In our previous investigations, we have reported the synthesis of both bulk and supported bimetallic Ni-Sn alloy catalysts from two types nickel precursors. *first*, from nickel salt (e.g., $NiCl_2$ or $NiCl_2 \cdot 4H_2O$) produced from both bulk and supported Ni-Sn alloys [11] and, *second*, from Raney® nickel supported on aluminium hydroxide (R-Ni/AlOH), which produced a nickel-tin alloy supported on aluminium hydroxide (Ni-Sn(*x*)/AlOH; x = Ni/Sn molar ratio) [12,13]. The catalysts showed high activity and selectivity during hydrogenation of F to FA [11–13], and the catalyst that consisted of the Ni_3Sn_2 alloy dispersed on TiO_2 allowed a remarkable reduction in the reaction temperature from 453 K to 383 K [11]. We have also recently reported the catalytic performance of the Ni-

* Corresponding authors.
E-mail addresses: rodiansono@unlam.ac.id (Rodiansono), shimazu@faculty.chiba-u.jp (S. Shimazu).

http://dx.doi.org/10.1016/j.mcat.2017.11.004
2468-8231/

Sn alloy during hydrogenation of biomass-derived levulinic acid in water to γ-valerolactone (GVL) [22,23]. Over bulk Ni-Sn alloy catalysts, a relatively high reaction temperature (433 K, 4.0 MPa H_2, 6 h) was applied to achieve both a high conversion and GVL yield (99%) [22]. Alternatively, a GVL yield of >99% was obtained over Ni-Sn(*x*)/AlOH catalysts at a lower reaction temperature (393 K) compared to the bulk catalysts [23]. We found that the selectivity of Ni could be controlled precisely by changing the Ni/Sn ratio in a Ni-Sn alloy or of the dispersion of the Ni-Sn alloy on an appropriate support that might play a key role in chemoselectivity enhancement.

Herein, we report our extended investigation on a facile and novel preparation method for nanosized bimetallic nickel-indium alloy catalysts supported on amorphous alumina (denoted Ni-In(*x*)/AA; *x* is Ni/In molar ratio and AA is amorphous alumina). Ni-In(*x*)/AA catalysts were synthesized via a very similar synthetic procedure to Ni-Sn(*x*)/AlOH, which has been reported elsewhere [12]. The effects of the loading amount of In and thermal treatment on the activity and selectivity of Ni-In(*x*)/AA catalysts during the hydrogenation of furfural to furfuryl alcohol were studied systematically.

2. Experimental

2.1. Reagents

Raney Ni-Al alloy (50%wt Ni and 50%wt Al) was purchased from Kanto Chemical Co., Inc.). NaOH, $InCl_3{\cdot}4H_2O$ and $SnCl_2{\cdot}2H_2O$ were purchased from WAKO Pure Chemical Industries, Ltd., and $GaCl_3$, $AgNO_3$, $NbCl_5$, and $ZrCl_4$ were purchased from Sigma-Aldrich, Co., and used as received. Furfural, furfuryl alcohol, tetrahydrofurfuryl alcohol, ethanol, and isopropanol were purchased from Tokyo Chemical Industries (TCI) Ltd. and purified using standard procedures prior to use.

2.2. Catalyst synthesis

2.2.1. Synthesis of R-Ni/AlOH

A typical procedure for the synthesis of the Raney nickel supported on aluminium hydroxide catalyst (denoted as R-Ni/AlOH) is described as follows [12,24]: Raney Ni-Al alloy powder (2.0 g) was slowly added to a dilute aqueous solution of NaOH (0.31 M, 16 mL) at room temperature. The temperature was raised to 363 K, and 4 mL of 3.1 M NaOH solution was subsequently added and stirred for 30 min. The mixture was then placed into a sealed Teflon autoclave reactor for hydrothermal treatment at 423 K for 2 h. The resulting precipitate was filtered, washed with distilled water until the filtrate was neutralized and then stored in water. Finally, the catalyst was dried under vacuum prior to use.

2.2.2. Synthesis of Ni-In/AlOH

A typical procedure for the synthesis of the nickel-indium alloy supported on aluminium hydroxide (denoted as Ni-In(*2.0*)/AlOH, 2.0 is Ni/In molar ratio) consisted of first mixing R-Ni/AlOH at room temperature in an ethanol/H_2O solution (~25 mL) that contained 4.5 mmol $InCl_3{\cdot}4H_2O$ and then stirring for 2 h. The mixture was placed into a sealed Teflon autoclave reactor for hydrothermal treatment at 423 K for 2 h. The resulting precipitate was filtered, washed with distilled water and ethanol, and dried under vacuum overnight. The Ni-In(*x*)/AlOH samples were reduced by hydrogen (H_2) at 673 K for 1.5 h, which produced Ni-In(*x*)/AA, where AA is amorphous alumina. The Ni-In(*2.0*)/AlOH sample was reduced by hydrogen (H_2) at 573–873 K for 1.5 h in order to investigate the effect of temperature reduction on the formation of the Ni-In alloy in Ni-In(*2.0*)/AA.

The H_2 uptake was determined through irreversible H_2 chemisorption. After the catalyst was heated at 393 K under vacuum for 30 min, it was then heated at 673 K under H_2 for 30 min. The catalysts were subsequently cooled to room temperature under vacuum for 30 min. The H_2 measurement was conducted at 273 K, and the H_2 uptake was calculated according to a method described in the literature [26,27].

2.3. Catalyst characterization

Powder X-ray diffraction (XRD) measurements were recorded on a Mac Science M18XHF instrument using monochromatic CuKα radiation (λ = 0.15418 nm). The XRD equipment operated at 40 kV and 200 mA with a step width of 0.02° and a scan speed of 4° min^{-1} (λ = 0.154057 nm, α2 = 0.154433 nm). Inductively coupled plasma (ICP) measurements were performed on an SPS 1800H plasma spectrometer by Seiko Instruments Inc., Japan (Ni: 221.7162 nm and Sn: 189.898 nm). The BET surface area (S_{BET}) and pore volume (V_p) were measured using N_2 physisorption at 77 K on a Belsorp Max (BEL Japan). The samples were degassed at 473 K for 2 h to remove physisorbed gases prior to the measurements. The amount of nitrogen adsorbed onto the samples was used to calculate the BET surface area via the BET equation. The pore volume was estimated to be the liquid volume of nitrogen at a relative pressure of approximately 0.995 according to the Barrett–Joyner–Halenda (BJH) approach based on desorption data [25]. SEM images of the synthesized catalysts were taken on a JEOL JSM-610 microscope after the samples were coated using a JEOL JTC-1600 autofine coater. TEM images were recorded on a JEOL JEM1400 microscope. Raman spectra were collected on a JASCO NRS-2100 laser-Raman spectrophotometer with an Ar beam lamp at excitations of 488 nm and 514.5 nm.

2.4. Typical procedure for the selective hydrogenation of furfural

The catalyst (50 mg), furfural (1.1 mmol), and isopropanol (3 mL) as the solvent were placed into a glass reaction tube, which fit inside a stainless steel reactor. After H_2 was introduced into the reactor at an initial H_2 pressure of 3.0 MPa at room temperature, the temperature of the reactor was increased to 383–453 K. After 75 min, the conversion of furfural (F) and the yields of furfuryl alcohol (FA) and tetrahydrofurfuryl alcohol (THFA) were determined using GC analysis. The used Ni-In(*2.0*)/AA 773 K/H_2 catalyst was easily separated using either simple centrifugation (4000 rpm for 10 min) or filtration, then finally dried overnight under vacuum at room temperature prior to re-usability testing.

2.5. Product analysis

GC analysis of the reactant (F) and products (FA and THFA) was performed on a Shimadzu GC-8A with a flame ionization detector equipped with a silicone OV-101 packed column (length (m) = 3.0; inner diameter (mm) = 2.0; methylsilicone from Sigma-Aldrich Co. Ltd.). Gas chromatography-mass spectrometry (GC–MS) was performed on a Shimadzu GC–17 B equipped with a thermal conductivity detector and an RT-βDEXsm capillary column. ^1H and ^{13}C NMR spectra were obtained on a JNM-AL400 spectrometer at 400 MHz; the samples for NMR analysis were dissolved in chloroform-d_1 with TMS as the internal standard. The products were confirmed by a comparison of their GC retention time, mass, ^1H and ^{13}C NMR spectra with those of authentic samples.

The conversion of furfural, yield and selectivity of the products were calculated according to the following equations:

$$\text{Conversion} : \frac{introduced\ mol\ reactant(F_0) - remained\ mol\ reactan(F_t)}{introduced\ mol\ reactant(F_0)} x100\%$$

$$\text{Yeild}: \frac{mol\ product}{consumed\ mol\ reactant\ (\Delta F)} x100\%$$

$$\text{Selectivity}: \frac{\boldsymbol{molproduct}}{\boldsymbol{total molproducts}} \boldsymbol{x}100\%$$

where F_0 is the introduced mol reactant (furfural, F), F_t is the remaining mol reactant, and ΔF is the consumed mol reactant (introduced mol reactant- remained mol reactant), which are all obtained from GC analysis using an internal standard technique.

3. Results and discussion

3.1. Catalyst characterization

A series of bimetallic alloys (Ni-In(x)/AA, x = Ni/In molar ratio) prepared via hydrothermal treatment of a mixture of Raney® nickel supported on aluminium hydroxide (R-Ni/AlOH) [12,24] and $InCl_2 \cdot H_2O$ solution in ethanol/H_2O at 423 K for 2 h, produced the *as-prepared* Ni-In(x)/AlOH. After reduction of the *as-prepared* Ni-In(x)/AlOH with H_2 treatment at 573–873 K for 1.5 h, Ni-In(x)/AA, x = Ni/In molar ratio and AA = amorphous alumina were produced. The physicochemical properties of the synthesized Ni-In(x)/AA catalysts are summarized in Table 1.

Based on the ICP-AES results, the loading amounts of In were 1.4, 2.3, 4.5, 6.2, and 9.4 mmol g^{-1}, which was reflected by the Ni/In molar ratios of 5.1, 3.1, 2.0, 1.1, and 0.8, respectively. The results also indicate that S_{BET} increased gradually, while the H_2 uptake decreased with an increase in the loading amount of In. The S_{BET} values of the Ni-In(x)/AA samples were higher than those of the as-prepared samples (Ni-In(x)/AlOH) because of thermal treatment or the formation of amorphous alumina. In the Ni-In(*2.0*)/AA sample, the H_2 uptake was 75 μmol g^{-1} (entry 4), which is comparable to the previous results of the H_2 uptake of Ni-Sn(*1.4*)/AlOH [12]. An increase in the loading amount of In reduced the surface activity of Ni, as also indicated by the H_2 uptake in samples with Ni/In ratios of 1.1-0.8 (entries 5–7) and bulk Ni-In(*2.0*) (entry 8).

The average crystallite sizes of the Ni(111) species or bimetallic Ni-In before and after H_2 treatment were calculated by using the Scherer equation using the diffraction peak at 2θ = 44.4° and the results are also summarized in Table 1. The findings indicate that the average crystallite sizes of Ni(111) or bimetallic Ni-In are larger than that of the as-prepared sample due to thermal treatment under hydrogen atmosphere. Compared with the bulk Ni-In(*2.0*) catalyst with average crystallite sizes of bimetallic Ni-In of 39.8 nm (entry 8), the crystallite sizes in Ni-In(x)/AA catalysts are much smaller. The crystallite sizes of Ni or the Ni-In alloy in Ni-In(x)/AA are also consistent with the H_2 uptake. These results suggest that the dispersion of active metal on amorphous alumina may influence the catalytic activity.

The XRD patterns of R-Ni/AlOH and the *as-prepared* Ni-In(x)/AlOH with different Ni/In molar ratios are shown in Fig. 1. R-Ni/AlOH showed sharp diffraction peaks at 2θ = 44.3°, 51.6°, and 76.3°, which correspond to the Ni(111), Ni(200), and Ni(220) species, respectively (Fig. 1**a**). Sharp diffraction peaks were also observed at 2θ = 18.3°, 27.8°, and 40.5°, which represent bayerite, and at 2θ = 18.7°, 20.4°, 36.7°, 37.8°, 53.2°, 63.9°, and 70.7°, which correspond to gibbsite (Fig. 1**a–f**). In contrast, the XRD patterns of the *as-prepared* Ni-In(x)/AlOH exhibited broadened peaks at 2θ = 44.4° due to the formation of bimetallic Ni-In, i.e., Ni_2In and Ni_3In_2 (Fig. 1**b–f**). The formation of bimetallic Ni_2In_3 (#JCPDS-36-1147) at 2θ = 31.9° and indium oxides such as In_2O_3 (#JCPDS-06-416) at 2θ = 22.4°, 39.4°, 51.0°, and 57.6° were also observed (**Figure d–f**) [24,28].

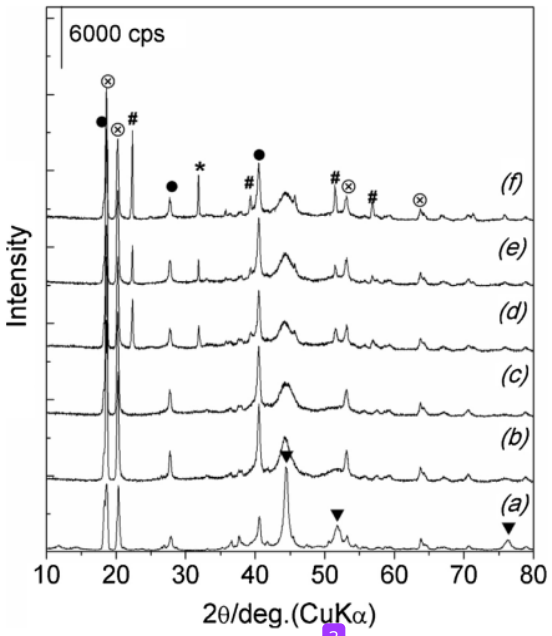

Fig. 1. XRD patterns of (a) R-Ni/AlOH and the *as-prepared* Ni-In(x)/AlOH (x = Ni/In molar ratio) at different Ni/In molar ratios of (b) 5.1, (c) 3.1, (d) 2.0, (e) 1.1, and (f) 0.8. (●) bayerite; (⊗) gibbsite; (#) $In(OH)_3$; (▼) Ni(0); (*) Ni_2In_3.

To confirm the formation of the bimetallic Ni-In alloy, the *as-prepared* Ni-In(x)/AlOH samples were reduced with H_2 at 673 K for 1.5 h and resulted in the bimetallic Ni-In alloy supported on amorphous alumina (denoted as Ni-In(x)/AA) and the XRD patterns are shown in Fig. 2.

The results indicate that controlled thermal treatment under H_2 transformed the remaining aluminium hydroxides (both bayerite and gibbsite phases) into amorphous alumina, which were not detectable using XRD analysis. The diffraction peak at 2θ = 44.4° that is recognized as an identical peak of the Ni(111) species became broadened and overlapped with the bimetallic Ni-In alloy phases with an increase in the loading amount of In (Fig. 2**a–e**). A shoulder peak at 2θ = 43.2° was also observed for a Ni/In ratio of 0.8 (where the amount of Ni »In) that can be attributed to the formation of the bimetallic Ni_3In species (#JCPDS-21-404) (Fig. 2**e**). Additionally, the broadened peak of the Ni(111) species both in the *as-prepared* and H_2-treated samples suggest the formation of a bimetallic Ni-In alloy that might have selectively occurred on the surface of Ni(111) rather than on the surface of Ni(200) or Ni(220) [29–31].

The low-frequency Raman spectrum of the *as-prepared* Ni-In(*2.0*)/AlOH resembles Ni-Sn(*1.4*)/AlOH, as has been previously reported [23]. It is found that the low-frequency Raman spectrum showed a 530 cm^{-1} band, which can be attributed to the γ(OH) vibrational mode and Al-O-Al deformation, whereas the 315 cm^{-1} band is ascribed to Al-O-Al stretching vibrations of gibbsite or bayerite (Fig. 3). Alternatively, the bands of Al-O-Al deformation and Al-O-Al stretching vibrations disappeared after H_2 treatment at 673 K for 1.5 h (Fig. 3**b**) due to the formation of amorphous alumina [32–34], which had been not detected by XRD [12,13]. Scanning electron microscopy (SEM) images, EDS spectra and TEM images of both Ni-In(*3.1*)/AA and Ni-In(*2.0*)/AA are shown in Figs. S1, S2, and S3 (see ESI), respectively.

Table 1
Physicochemical properties of the synthesized bimetallic Ni-In alloy catalysts supported on amorphous alumina (Ni-In(*x*)/AA, *x* = Ni/In molar ratio).

Entry	Catalysts[a]	Ni[a]	In[a]	H_2 uptake[b]/	S_{BET}[c]/	D[d]/nm
		(mmol^{-1})	(mmol^{-1})	μmol g^{-1}	m^2 g^{-1}	
1	Raney Ni	4.0	0	121	70	8.6
2	R-Ni/AlOH	3.5	0	104	150	9.0
3	Ni-In(*5.1*)/AA	7.1	1.4	84	128(101)	8.0(5.2)
4	Ni-In(*3.1*)AA	7.2	2.3	71	120(90)	7.0(3.8)
5	Ni-In(*2.0*)/AA	8.8	4.5	75	154(98)	3.8(2.9)
6	Ni-In(*1.1*)/AA	7.0	6.2	76	161(75)	6.6(3.9)
7	Ni-In(*0.8*)/AA	7.2	9.4	48	157(72)	5.2(3.4)
8[e]	Bulk Ni-In(*2.0*)	4.1	2.0	29	43	39.8

[a] Values between parentheses are the Ni/In molar ratios determined by ICP-AES.
[b] Based upon the total H_2 uptake at 273 K (after corrections for physical and chemical adsorption).
[c] Specific surface area of BET (S_{BET}) of samples after H_2 treatment at 673 K for 1.5 h, determined by N_2 adsorption at 77 K; values between parentheses are the S_{BET} values of the as-prepared samples.
[d] Average Ni(111) or Ni-In crystallite sizes were calculated according to the Scherer equation; values between parentheses are the crystallite sizes of Ni(111) or Ni-In of the as-prepared catalysts.
[e] Bulk Ni-In(*2.0*) catalysts were synthesized via the hydrothermal treatment of a mixture of $NiCl_2$ and $InCl_3{\cdot}4H_2O$ solutions at 423 K for 24 h, followed by H_2 treatment at 673 K for 1.5 h.

3.2. Catalytic reactions: furfural hydrogenation

3.2.1. Selection of the second metals

At the first stage, the catalytic performances of various transition metal modified-R-Ni/AlOH, such as Sn, In, Ga, Ag, Nb, and Zr, were first evaluated by the selective hydrogenation of the typical unsaturated aldehyde furfural (F) to furfuryl alcohol (FA), which is a promising chemical intermediate for the synthesis of biosourced products widely used in the polymer industry. Conventional Raney nickel (Raney Ni) and Raney nickel supported on aluminium hydroxide (R-Ni/AlOH) catalysts were also synthesized and evaluated using the same reaction conditions as catalyst references. The detailed information for these catalysts is summarized in Table S1 in the ESI. The XRD patterns of the as-prepared R-Ni-M/AlOH are shown in Fig. S4 in the ESI. The results of the catalytic hydrogenation of F are summarized in Table 2, and the reaction pathways are shown in Scheme 1.

Conventional Raney Ni exhibited a 99.6% conversion of F and FA and THFA yields of 48% and 51%, respectively (entry 1). As expected, by using the R-Ni/AlOH catalyst, F converted completely to produce a 99% yield of THFA (entry 2). Interestingly, the addition of Sn or In shifted the product selectivity to FA with yields of 91% and 40%, respectively (entries 3 and 4). In tin-alloyed Ni-based (Ni-Sn) catalysts, the catalytic performances have been reported previously [11–13,22,23]. Alternatively, the presence of Ga, Ag, and Nb significantly reduced the activity of R-Ni/AlOH (entries 5, 6, and 7), while Zr did not affect the activity or selectivity of the former catalyst (entry 8). Therefore, in the present report, we focused on catalytic performance studies of indium-alloyed Ni catalysts on F hydrogenation including the effect of loading amount, H_2 treatment, time profiles, and catalyst reusability.

3.2.2. Effect of In loading amount

The results for the selective hydrogenation of F using the as-prepared supported bimetallic Ni-In(*x*)/AlOH catalysts are summarized in Table 3.

It can be observed that after introducing 1.4 mmol $InCl_3{\cdot}4H_2O$ to R-Ni/AlOH, the conversion of F drastically decreased to 47% and yielded 40% FA (entry 1). By increasing the loading amount of In to 9.4 mmolg^{-1}, the FA yield was almost constant (entries 7 and 8, 51% and 39%, respectively). The prolonged reaction time of 180 min over Ni-In(*2.0*)/AlOH produced a marked increase in the FA yield from 55% to 92% (entries 3 and 4, respectively). In contrast, the yield of tetrahydrofurfuryl alcohol (THFA) decreased to 4% (entry 4). The FA yield decreased when an initial H_2 pressure of 2.0 MPa was applied (entry 5, 40%). The F conversion and FA yield drastically decreased without the presence of H_2 (entry 6). The R-Ni-In/SiO_2 catalyst (loading amount of In, 2.7 mmolg^{-1}) produced a 43% conversion and a 39% yield of FA (entry 9). Moreover, the In/AlOH, In_2O_3, and $InCl_3{\cdot}4H_2O$ catalysts (entries 10–12) and the absence of a catalyst (entry 13) did not produce hydrogenated products of F under the same conditions. In addition, screening tests using solvents (e.g., methanol, ethanol, toluene, 1-propanol, and H_2O) other than isopropanol (*iso*-PrOH) were also performed, and the results were inferior to the results with *iso*-PrOH, as reported previously [35].

The H_2 treatment of as-prepared Ni-In(*x*)/AlOH at 673 K for 1.5 h resulted in Ni-In(*x*)/AA catalysts (the XRD patterns are shown in Fig. 2). The catalysts were evaluated for the catalytic hydrogenation of biomass-derived furfural to furfuryl alcohol, and the results are summarized in Table 4. Interestingly, over H_2-treated Ni-In(*x*)/AA catalysts, the high conversion of F was achieved and produced a high yield of FA (entries 1–6). In Ni-In(*2.0*)/AA, F was converted completely into almost a 100% yield of FA. The high yield of FA without the formation of THFA, even though the reaction time was prolonged to 360 min (entry 4), obviously indicated the important role of In in the Ni-In alloy catalyst system. Additionally, over the indium-modified Raney Ni supported on silica (RNi-In/SiO_2 673 K/H_2) catalyst, the conversion of F was 96% with yield of FA that was much lower than that of Ni-In(*2.0*)/AA under the same reaction conditions (entry 7). The XRD patterns of this catalyst are shown in Fig. S5 in the ESI, and the physicochemical properties are summarized in Table S1 in the ESI. Moreover, by using the bulk Ni-In(*2.0*) catalyst (XRD patterns are shown in Fig. S6 in the ESI), the conversion of F was only 42% under the same reaction conditions (entry 8).

3.2.3. Effect of thermal treatment on Ni-In(2.0)/AlOH catalysts

Among the synthesized Ni-In(*x*)/AA catalysts, Ni-In(*2.0*)/AA demonstrated a very high activity and selectivity towards the desired product of FA. Therefore, we investigated the effect of temperature during hydrogen treatment on Ni-In(*2.0*)/AA at 573–873 K for 1.5 h, and the XRD patterns are shown in Fig. 4. After H_2 treatment at 573 K, the diffraction peaks of the aluminium hydroxides (e.g., bayerite and gibbsite) totally disappeared, and the broadened peaks at 2θ = 42-44.5° were hardly distinguished due to the overlap of the bimetallic alloy Ni-In phases and Ni metal diffraction peaks. Peak formation of NiIn (PDF#07-0178) at 2θ = 30.2° and the remaining In_2O_3 at 2θ = 22.3° and 31.9° was clearly observed (Fig. 4**a-b**). The increase in temperature from 673 K to 873 K transformed the NiIn alloy species to Ni_3In (PDF #65-3486), Ni_3In (PDF#65-3522)

Table 2
Results of the catalytic hydrogenation of biomass-derived furfural over the various *as-prepared* bimetallic Ni-M/AlOH catalysts (M = Sn, In, Ga, Ag, Nb, and Zr).

Entry	Catalyst	M[a] /mmol g^{-1}	Conversion[b]/%	Yield[b]/%	
				FA	THFA
1	Raney Ni	–	99	48	51
2	R-Ni/AlOH	–	>99	1	99
3	Ni-Sn/AlOH	1.0	95.0	91	3
4	Ni-In/AlOH	1.4	47.0	40	7
5	Ni-Ga/AlOH	1.1	12.8	0	0
6	Ni-Ag/AlOH	1.2	44.9	7	16
7	Ni-Nb/AlOH	1.2	47.3	6	17
8	Ni-Zr/AlOH	1.1	>99	0	96

Reaction conditions: catalyst (50 mg), F (1.1 mmol), *iso*-PrOH (3 mL), H_2 (3.0 MPa), 453 K, 75 min.
[a] Loading amount of In was determined by ICP-AES.

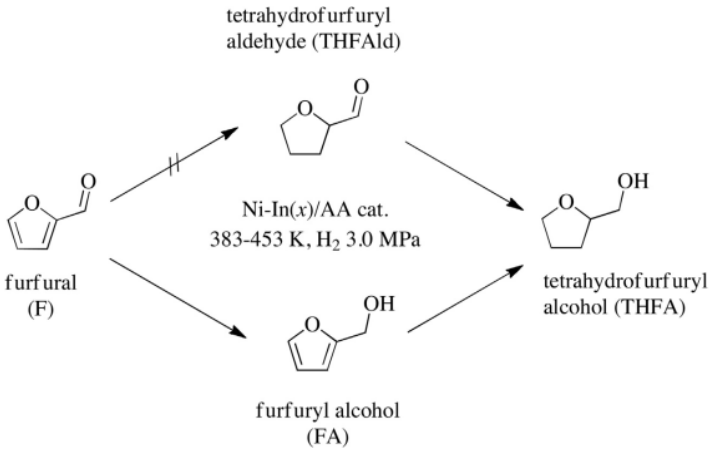

Scheme 1. Reaction pathways of furfural hydrogenation over bimetallic Ni-In catalysts.

Table 3
Results of the catalytic hydrogenation of biomass-derived furfural over *as prepared* bimetallic Ni-In(*x*)/AlOH catalysts with various loading amounts of indium (In).

Entry	Catalyst[a]	In[b] /mmol g^{-1}	Conversion[c]/%	Yield[c]/%	
				FA	THFA
1	Ni-In(*5.1*)/AlOH	1.4	47	40	7
2	Ni-In(*3.1*)/AlOH	2.3	53	47	6
3	Ni-In(*2.0*)/AlOH	4.5	61	55	6
4[d]	Ni-In(*2.0*)/AlOH	4.5	96	92	4
5[e]	Ni-In(*2.0*)/AlOH	4.5	45	40	5
6[f]	Ni-In(*2.0*)/AlOH	4.5	17	5	2
7	Ni-In(*1.1*)/AlOH	6.2	59	51	8
8	Ni-In(*0.8*)/AlOH	9.4	42	39	3
9[g]	R-Ni-In/SiO_2	2.7	43	39	4
10	In/AlOH	4.5	28	0	0
11	In_2O_3	–	28	6	3
12	$InCl_3{\cdot}4H_2O$	–	52	3	1
13	Neat (no catalyst)	–	15	0	0

Values between parentheses are the Ni/In molar ratio. *Reaction conditions:* catalyst (50 mg), F (1.1 mmol), *iso*-PrOH (3 mL), H_2 (3.0 MPa), 453 K, 75 min.
[b] Loading amount of In was determined by ICP-AES.
[c] Conversion and yield were determined by GC analysis using an internal standard.
[d] Reaction time was 180 min.
[e] Initial pressure of H_2 was 2.0 MPa.
[f] Reaction occurred in the absence of H_2.
[g] Precursor of nickel was Raney Ni and supported on SiO_2.

and Ni_2In_3 (PDF # 65–3486) alloy phases (Fig. 4c–e), and the peaks became intensified at a temperature of 873 K (Fig. 4**e**).

The results of the catalytic hydrogenation of F to FA and THFA over Ni-In(2.0)/AA treated with H_2 at different temperature treatments are summarized in Table 5. For Ni-In(*2.0*)/AA catalysts at 573 K (entry 1) and 673 K (entry 2), a small amount of THFA product was obtained over those catalysts (5% and 1% yield of THFA, respectively). The best catalytic performance was achieved over Ni-In(*2.0*)/AA 773 K (entry 3) and Ni-In(*2.0*)/AA 873 K (entry 4). We also intentionally carried out the hydrogenation reaction of FA as substrate over Ni-In(*2.0*)/AA 773 K under the same reaction conditions, and only 5.2% of FA was converted into THFA with a yield of

Table 4
Results of the catalytic hydrogenation of biomass-derived furfural over bimetallic Ni-In(*x*)/AA catalysts after H_2 treatment at 673 K for 1.5 h.

Entry	Catalyst[a]	In[b]/mmolg^{-1}	Conversion[c]/%	Yield[c]/%	
				FA	THFA
1	Ni-In(*5.1*)/AA	1.4	98	94	4
2	Ni-In(*3.1*)/AA	2.3	97	95	2
3	Ni-In(*2.0*)/AA	4.5	>99	100	0
4[d]	Ni-In(*2.0*)/AA	4.5	>99	99	1
5	Ni-In(*1.1*)/AA	6.2	99	96	3
6	Ni-In(*0.8*)/AA	9.4	97	93	4
7	RNi-In/SiO_2	2.7	96	87	9
8[e]	Bulk Ni-In(*2.0*)	2.0	42	42	0

Values between parentheses are the Ni/In molar ratio. *Reaction conditions:* catalyst (50 mg), F (1.1 mmol), *iso*-PrOH (3 mL), H_2 (3.0 MPa), 453 K, 75 min.
[a] Loading amount of In was determined by ICP-AES.
[c] Conversion and yield were determined by GC analysis using an internal standard.
[d] Reaction time was 360 min.
[e] Bulk Ni-In(*2.0*) catalyst was synthesized via hydrothermal treatment of $NiCl_2$ and $InCl_3{\cdot}4H_2O$ in an ethanol/H_2O mixture at 423 K for 2 h, subsequently followed by reduction with H_2 at 673 K for 1.5 h. The XRD patterns of the as-prepared and H_2-treated bulk Ni-In(*2.0*) samples are shown in Fig. S6 in the ESI.

Table 5
Results of furfural hydrogenation over various Ni-In(*2.0*)/AA catalysts after H_2 treatment at various temperature of 573–873 K for 1.5 h.

Entry	Catalyst	Temp. H_2 treatment/K	Conversion[a]/%	Yield[a]/%	
				FA	THFA
1	Ni-In(*2.0*)/AA	573	>99	95.0	5.0
2	Ni-In(*2.0*)/AA	673	>99	99.0	1.0
3	Ni-In(*2.0*)/AA	773	>99	99.9	0
4	Ni-In(*2.0*)/AA	873	>99	99.9	0
5[b]	Ni-In(*2.0*)/AA	773	5	–	5.0

Reaction conditions: catalyst (50 mg), furfural (1.1 mmol), *iso*-PrOH (3 mL), H_2 3.0 MPa, 453 K, 75 min.
[a] Conversion and yield were determined by GC analysis using an internal standard.
[b] Furfuryl alcohol (FA) was the substrate, and reaction time was 180 min.

5%, even after the reaction time was prolonged to 180 min (entry 5). These results suggest that the addition of indium to R-Ni/AlOH to form the bimetallic Ni-In alloy retards the C=C hydrogenation activity of nickel, and as a result, further hydrogenation of the C=C furan ring in F did not proceed in the presence of the Ni-In(*2.0*)/AA catalyst.

3.2.4. Effect of temperature

The effect of temperature on the catalytic hydrogenation of F to FA was evaluated over both Ni-In(*2.0*)/AA 773 K/H_2 and bulk Ni-In(*2.0*) catalysts, and the results are shown in Fig. 5. Differences in the activity of each catalyst were clearly observed. On the bulk Ni-In(*2.0*) catalyst, the conversion of F gradually increased as temperature increased, and the highest conversion of F (~76%) was achieved at 453 K at the current reaction conditions. In contrast, F was converted completely at 443 K over the Ni-In(*2.0*)/AA 773 K/H_2 catalyst. These results are very similar to the bimetallic Ni-Sn alloy catalyst system, in which bulk Ni-Sn catalysts have much lower activity and reactivity during F hydrogenation compared with the supported Ni-Sn catalysts, as reported previously [11].

3.2.5. Effect of initial H_2 pressure

The effect of the initial H_2 pressure on F conversion and product selectivity was evaluated over the Ni-In(*2.0*)/AA 773 K/H_2 catalyst, and the results are shown in Fig. 6. F conversion and FA selectivity gradually increased as the initial H_2 pressure increased, whereas the THFA selectivity decreased smoothly to almost 0% between 2.5 and 3.0 MPa and then gradually increased between 3.5–4.0 MPa.

3.2.6. Kinetics

The kinetics of F hydrogenation at 453 K on the bulk and supported Ni-In(*2.0*)/AA 773 K/H_2 alloy catalysts are shown in Fig. 7. When the bulk Ni-In(*2.0*) catalyst was used, FA was slowly

Table 6
Results of the re-usability tests for the Ni-In(*2.0*)/AA 773 K/H_2 catalyst in the selective hydrogenation of furfural.

Run[a]	1	2	3	4	5
Conversion (%)	>99	95	93	91	91
Selectivity[b](%)	100	99	99	99	99

Reaction conditions: F, 1.1 mmol (F/Ni ratio = 15); *iso*-PrOH (3 mL); H_2, 3.0 MPa, 453 K, 75 min.
[a] The recovered catalyst was reused without any further treatment.
[b] Selectivity to FA was determined by GC analysis using an internal standard technique.

increased to achieve a 75% yield, even after 180 min. Therefore, a similar explanation can be applied to the current results as follows. The induction periods could be associated with the slow formation of oxidic tin (Sn^{n+}) from metallic tin (Sn^0), as reported by Sordelli et al. (Rh-Sn) [36] and Margitfalvi et al. (Pt-Sn) [37]. Since the crystallite size or dispersion of Ni-In alloy could affect the length of the induction period, the induction period of Ni-In(*2.0*)/AA diminished, and a 100% F conversion (>99% FA yield) was achieved after 75 min. The excellent catalytic performance of Ni-In(*2.0*)/AA produces a promising candidate suitable for the large-scale production of FA from the selective hydrogenation of furfural (F).

3.2.7. Re-usability test

A re-usability test was performed on the Ni-In(*2.0*)/AA 773 K/H_2 catalyst, and the results are summarized in Table 6.

The used Ni-In(*2.0*)/AA catalyst was easily separated by either simple centrifugation or filtration after the reaction. The activity of the catalyst slightly decreased, while a high selectivity was maintained for at least five consecutive runs. The amount of Ni and In that leached into the reaction solution was 0.7% and 1.4%, respectively, after four runs. The small amount of leached metal is consistent with the XRD patterns of the recovered Ni-In(*2.0*)/AA 773 K/H_2 cata-

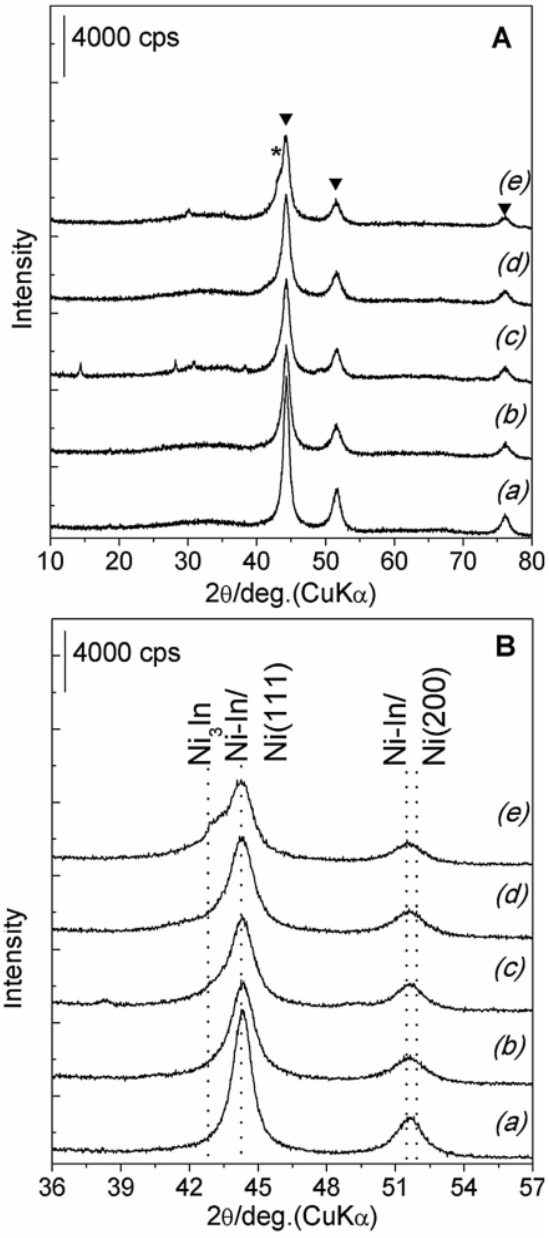

Fig. 2. XRD patterns of the H_2-treated Ni-In(*x*)/AA at a temperature of 673 K for 1.5 h and selected area at 2θ = 40–50° for (a) 5.1, (b) 3.1, (c) 2.0, (d) 1.1, and (e) 0.8. (▼) Ni(0); (*) bimetallic Ni_3In (#JCPDS-21-404).

lyst, and no obvious phase separation or agglomeration of the Ni_2In nanoparticles was observed in the used Ni-In(*2.0*)/AA 773 K/H_2 catalyst as indicated by the XRD patterns (Fig. S7 in the ESI).

4. Conclusions

A novel preparation method for bimetallic nickel-indium alloy catalysts supported on amorphous alumina (Ni-In(*x*)/AA; *x* = Ni/In molar ratio) catalysts has been developed and evaluated for the

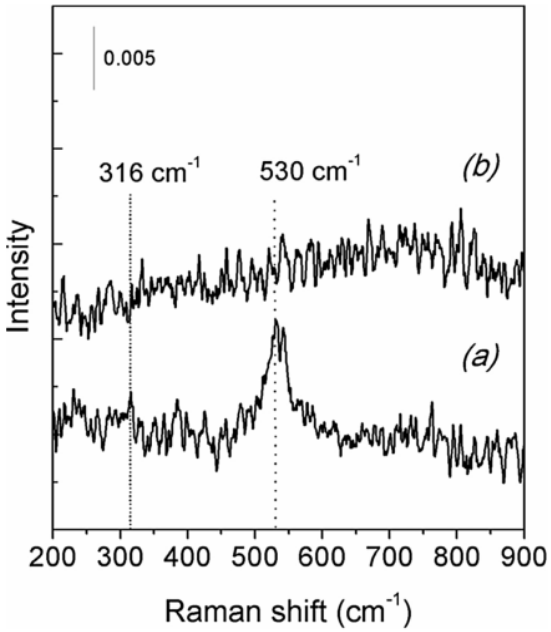

Fig. 3. Raman spectra of (a) the as-prepared Ni-In(*2.0*)/AlOH and (b) after H_2 treatment at 673 K for 1.5 h (Ni-In(*2.0*)/AA)).

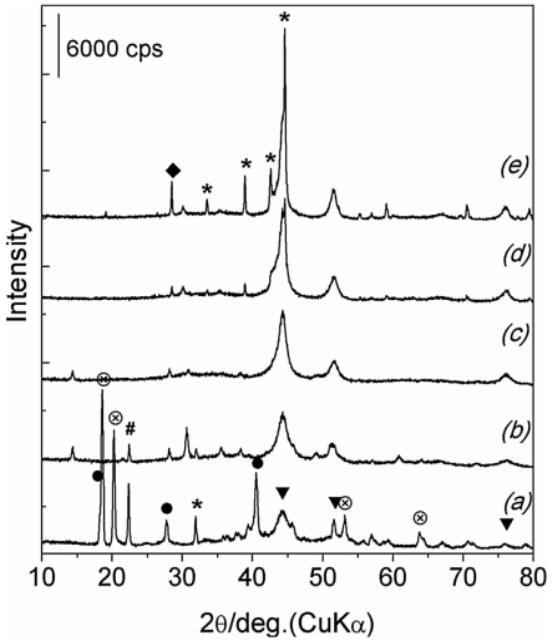

Fig. 4. XRD patterns of (a) *as-prepared* Ni-In(*2.0*)/AlOH and H_2 treated (Ni-In(*2.0*)/AA) at different temperatures of (b) 573, (c) 673, (d) 773, and (e) 873 K for 1.5 h. (●) bayerite; (⊗) gibbsite; (#) $In(OH)_3$; (▼) Ni(0); (*) Ni_3In (#JCPDS-21-404); (♦) Ni_2In_3 (#JCPDS-65-3486).

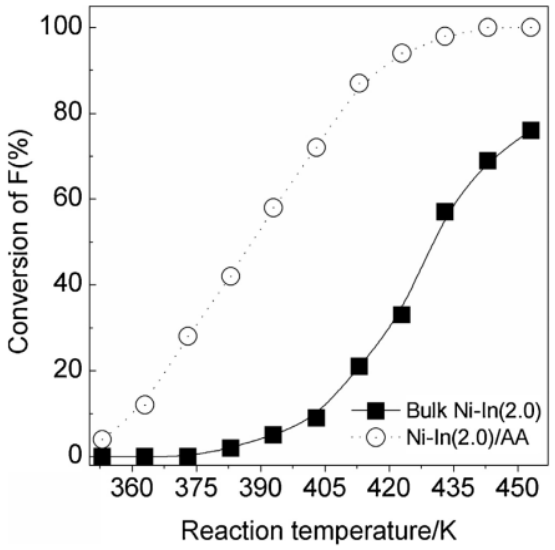

Fig. 5. Effect of reaction temperature on the conversion of furfural (F) over the bulk and supported Ni-In(*2.0*)/AA 773 K/H_2 alloy catalysts. *Reaction conditions:* catalyst, 50 mg; F, 1.1 mmol; *iso*-PrOH, 3 mL; H_2, 3.0 MPa, 75 min.

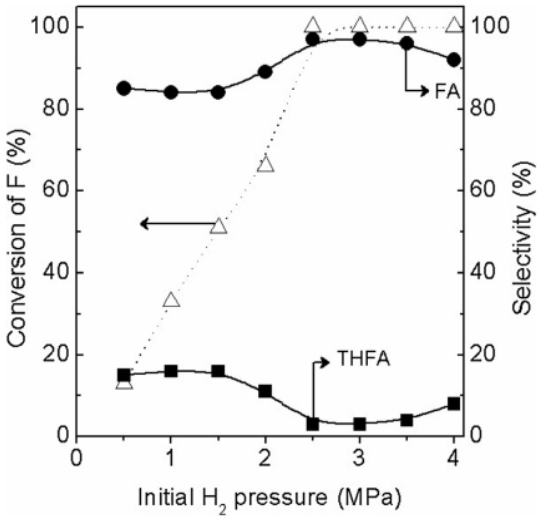

Fig. 6. Effect of the initial H_2 pressure on the conversion and selectivity in the hydrogenation of furfural (F) over the Ni-In(*2.0*)/AA 773 K/H_2 alloy catalyst. *Reaction conditions:* catalyst, 50 mg; F, 1.1 mmol; isoPrOH, 3 mL; 453 K, 75 min.

highly selective hydrogenation of biomass-derived furfural. The formation of Ni-In alloy phases such as Ni_3In_2, Ni_3In, and Ni_2In in Ni-In(*2.0*)/AA was clearly observed after H_2 treatment at 773 K for 1.5 h. Ni-Sn(*2.0*)/AA contained an Ni_2In alloy as the major phase, which exhibited the best catalytic performance for the selective hydrogenation of furfural to furfuryl alcohol exclusively and was stable for at least five consecutive reaction runs.

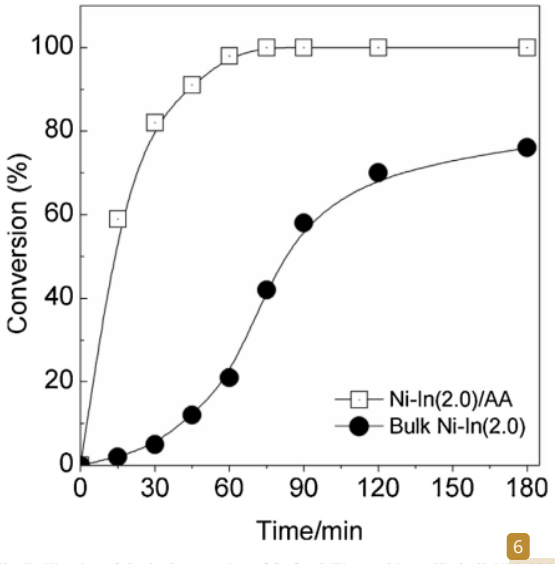

Fig. 7. Kinetics of the hydrogenation of furfural (F) over bimetallic bulk Ni-In(*2.0*) and Ni-In(*2.0*)/AA catalysts. *Reaction conditions:* catalyst, 50 mg; F, 1.1 mmol; *iso*-PrOH, 3 mL; H_2, 3.0 MPa, 453 K.

Acknowledgements

This work was financially supported by JPS-DGHE through the Joint Bilateral Research Project FY 2014-2017, KLN and the International Publication Project of DGHE FY 2016 under Grant Number of DIPA-023-04.1.673453/2016, Insentif Riset Nasional (Insinas) FY 2016-2017, and IPTEKS Project FY 2016, Ministry of Research, Technology & Higher Education, Republic of Indonesia.

Appendix A. Supplementary data

Supplementary data associated with this article can be found, in the online version, at http://dx.doi.org/10.1016/j.mcat.2017.11.004.

References

[1] J. Falbe, H. Bahrmann, W. Lipps, D. Meyer, Ullmanns Encyclopedia of Industrial Chemistry, 11, Wiley-VCH Verlag GmbH & Co., 2005, pp. 21.
[2] J.P. Lange, E. van der Heide, J. van Buijtenen, R. Price, Furfural a promising platform for lignocellulosic biofuels, ChemSusChem 5 (2012) 150–166, http://dx.doi.org/10.1002/cssc.201100648.
[3] R. Mariscal, P. Maireles-Torres, M. Ojeda, I. Sádaba, M.L. Granados, Furfural: a renewable and versatile platform molecule for the synthesis of chemicals and fuels, Energy Environ. Sci. 9 (2016) 1144–1189, http://dx.doi.org/10.1039/C5EE02666K.
[4] P. Gallezot, Conversion of biomass to selected chemical products, Chem. Soc. Rev. 41 (2012) 1538–1558, http://dx.doi.org/10.1039/C1CS15147A.
[5] S. Dutta, S. De, B. Saha, Md. I. Alam, Advances in conversion of hemicellulosic biomass to furfural and upgrading to biofuels, Catal. Sci. Technol. 2 (2012) 2025–2036, http://dx.doi.org/10.1039/c2cy20235b.
[6] P.S. Metkar, E.J. Till, D.R. Corbin, C.J. Pereira, K.W. Hutchenson, S.K. Sengupta, Reactive distillation process for the production of furfural using solid acid catalysts, Green Chem. 17 (2015) 1453–1466, http://dx.doi.org/10.1039/C4GC01912A.
[7] D.M. Alonso, S.G. Wettstein, J.A. Dumesic, Bimetallic catalysts for upgrading of biomass to fuels and chemicals, Chem. Soc. Rev. 41 (2012) 8075–8098, http://dx.doi.org/10.1039/C2CS35188A.
[8] J. Pritchard, G.A. Filonenko, R. van Putten, E.J.M. Hensen, E.A. Pidko, Heterogeneous and homogeneous catalysis for the hydrogenation of carboxylic acid derivatives: history, advances and future directions, Chem. Soc. Rev. 44 (2015) 3808–3833, http://dx.doi.org/10.1039/C5CS00038F.
[9] M. Besson, P. Gallezot, C. Pine, Conversion of biomass into chemicals over metal catalysts, Chem. Rev. 114 (2014) 1827–1870, http://dx.doi.org/10.1021/cr4002269.
[10] J.G.M. Bremner, R.K.F. Keeys, The hydrogenation of furfuraldehyde to furfuryl alcohol and sylvan (2-methylfuran), J. Chem. Soc. (1947) 1068–1080, http://dx.doi.org/10.1039/JR9470001068.
[11] Rodiansono, S. Khairi, T. Hara, N. Ichikuni, S. Shimazu, Highly efficient and selective hydrogenation of unsaturated carbonyl compounds using Ni-Sn

alloy catalysts, Catal. Sci. Technol. 2 (2012) 2139–2145, http://dx.doi.org/10.1039/C2CY20216F.
[12] Rodiansono, T. Hara, T. Ichikuni, S. Shimazu, A novel preparation method of Ni-Sn alloy catalysts supported on aluminium hydroxide: application to chemoselective hydrogenation of unsaturated carbonyl compounds, Chem. Lett. 41 (2012) 769–771, http://dx.doi.org/10.1246/cl.2012.769.
[13] Rodiansono, T. Hara, N. Ichikuni, S. Shimazu, Development of nanoporous Ni-Sn alloy and application for chemoselective hydrogenation of furfural to furfuryl alcohol, Bull. Chem. React. Eng. Catal. 9 (1) (2014) 53–59, http://dx.doi.org/10.9767/bcrec.9.1.5529.53-59.
[14] A. Halilu, T.H. Ali, A.Y. Atta, P. Sudarsanam, S.K. Bhargava, S. bee abd hamid, highly selective hydrogenation of biomass-Derived furfural into furfuryl alcohol using a novel magnetic nanoparticles catalyst, Energy Fuels 30 (3) (2016) 2216–2226, http://dx.doi.org/10.1021/acs.energyfuels.5b02826.
[15] W.S. Putro, T. Hara, N. Ichikuni, S. Shimazu, Efficiently recyclable and easily separable Ni-Fe alloy catalysts for chemoselective hydrogenation of biomass-derived furfural, Chem. Lett. 46 (1) (2017) 149–151, http://dx.doi.org/10.1246/cl.160905.
[16] C. Li, Y. Chen, S. Zhang, S. Xu, J. Zhou, F. Wang, M. Wei, D.G. Evans, X. Duan, Ni–In intermetallic nanocrystals as efficient catalysts toward unsaturated aldehydes hydrogenation, Chem. Mater 25 (2013) 3888–3896, http://dx.doi.org/10.1021/cm4021832.
[17] S. Sitthisa, W. An, D.E. Resasco, Selective conversion of furfural to methylfuran over silica-supported Ni-Fe bimetallic catalysts, J. Catal. 284 (2011) 90–101, http://dx.doi.org/10.1016/j.jcat.2011.09.005.
[18] D. Shi, J.M. Vohs, Deoxygenation of biomass-Derived oxygenates: reaction of furfural on Zn-Modified Pt(111), ACS Catal. 5 (2015) 2177–2183, http://dx.doi.org/10.1021/acscatal.5b00038.
[19] F. Delbecq, P. Sautet, Competitive CC and CO adsorption of α-β- unsaturated aldehydes on Pt and Pd surfaces in relation with the selectivity of hydrogenation reactions: a theoretical approach, J. Catal. 152 (1995) 217–236, http://dx.doi.org/10.1006/jcat.1995.1077.
[20] F. Delbecq, P. Sautet, Influence of Sn additives on the selectivity of hydrogenation of α-β-unsaturated aldehydes with Pt catalysts: a density functional study of molecular adsorption, J. Catal. 220 (2003) 115–126, http://dx.doi.org/10.1016/S0021-9517(03)002495.
[21] V. Hlukhyy, F. Raif, P. Clauss, T.F. Fässler, Polar intermetallic compounds as catalysts for hydrogenation reactions: synthesis, structures, bonding, and catalytic properties of $Ca_{1-x}SrxNi_4Sn_2$ (x = 0. 0, 0. 5, 1. 0) and catalytic properties of Ni_3Sn and Ni_3Sn_2, Chem. Eur J. 14 (2008) 3737–3744, http://dx.doi.org/10.1002/chem.200701547.
[22] Rodiansono, A. Ghofur, M.D. Astuti, K.C. Sembiring, Catalytic hydrogenation of levulinic acid in water into γ-Valerolactone over bulk structure of inexpensive intermetallic Ni-Sn alloy catalysts, Bull. Chem. React. Eng. Catal. 10 (2) (2015) 192–200, http://dx.doi.org/10.9767/bcrec.10.2.8284.192-200.
[23] Rodiansono, M.D. Astuti, T. Hara, N. Ichikuni, S. Shimazu, Efficient hydrogenation of levulinic acid in water using a supported Ni-Sn alloy on aluminium hydroxide catalysts, Catal. Sci. Technol. 6 (2016) 2955–2961, http://dx.doi.org/10.1039/c5cy01731a.
[24] J. Petro, A. Bota, K. Laszlo, H. Beyer, E. Kalman, I. Dódony, A new alumina-supported, not pyrophoric Raney-type Ni catalyst, Appl. Catal. A 190 (2000) 73–86, http://dx.doi.org/10.1016/S0926-860X(99)00267-7.
[25] S. Lowell, J.E. Shields, M.A. Thomas, M. Thommes, Characterization of Porous Solids and Powders: Surface Area, Pore Size and Density Chapter 8, Kluwer Academic Publishers, Netherlands, 2004.
[26] C.H. Bartholomew, R.B. Pannel, J.L. Butler, Support and crystallite size effects in CO hydrogenation on nickel, J. Catal. 65 (1980) 335–347, http://dx.doi.org/10.1016/0021-9517(80)90311-5.
[27] C.H. Bartholomew, R.B. Pannel, The stoichiometry of hydrogen and carbon monoxide chemisorption on alumina- and silica-supported nickel, J. Catal. 65 (1980) 390–401, http://dx.doi.org/10.1016/0021-9517(80)90316-4.
[28] Powder Diffraction Files, JCPDS-International Centre for Diffraction Data (ICDD), 1997.
[29] H.E. Swift, J.E. Bozik, Metallic phases and activities of nickel-tin-silica catalysts: dehydrogenation of cyclohexanone, cyclohexanol, and cyclohexane, J. Catal. 12 (1968) 5–14, http://dx.doi.org/10.1016/0021-9517(68)90067-5.
[30] E. Nikolla, J. Schwank, S. Linic, Promotion of the long-term stability of reforming Ni catalysts by surface alloying, J. Catal. 250 (2007) 85–93, http://dx.doi.org/10.1016/j.jcat.2007.04.020.
[31] R. Sun, M. Zheng, J. Pang, X. Liu, J. Wang, X. Pan, A. Wang, X. Wang, T. Zhang, Selectivity-Switchable conversion of cellulose to glycols over Ni–Sn catalysts, ACS Catal. 6 (2016) 191–201, http://dx.doi.org/10.1021/acscatal.5b01807.
[32] H.D. Ruan, R.L. Frost, J.T. Kloprogge, Comparison of Raman spectra in characterizing gibbsite, bayerite, diaspore and boehmite, J. Raman Spectros. 32 (9) (2001) 745–750, http://dx.doi.org/10.1002/jrs.736.
[33] H.D. Ruan, R.L. Frost, J.T. Kloprogge, L. Duong, Far-infrared spectroscopy of alumina phases, Spectrochimica Acta Part A 58 (2002) 265–272, http://dx.doi.org/10.1016/S1386-1425(01)00532-7.
[34] S. Cava, S.M.n-name>J.T. Kloprogge, L. Duong, Far-infrared spectroscopy of alumina phases, Spectrochimica Acta Part A 58 (2002) 265–272, http://dx.doi.org/10.1016/S1386-1425(01)00532-7.
[34] S. Cava, S.M. Tebcherani, I.A. Souza, S.A. Pianaro, C.A. Paskocimas, E. Longo, J.A. Varela, Structural characterization of phase transition of Al_2O_3 nanopowders obtained by polymeric precursor method, Mater. Chem. Physics 103 (2007) 394–399, http://dx.doi.org/10.1016/j.matchemphys.2007.02.046.
[35] Rodiansono, M.D. Astuti, U.T. Santoso, S. Shimazu, Hydrogenation of biomass-derived furfural over highly dispersed-Aluminium hydroxide supported Ni-Sn(3.0) alloy catalysts, Procedia Chem. 16 (2015) 531–539, http://dx.doi.org/10.1016/j.proche.2015.12.089.
[36] L. Sordelli, R. Psaro, G. Vlaic, A. Cepparo, S. Recchia, A. Fusi, R. Zanoni, EXAFS studies of supported Rh–Sn catalysts for citral hydrogenation, J. Catal. 182 (1999) 186–198, http://dx.doi.org/10.1006/jcat.1998.2348.
[37] J.L. Margitfalvi, A. Tompos, I. Kolosova, J. Valyon, Reaction induced selectivity improvement in the hydrogenation of crotonaldehyde over Sn-Pt/SiO_2 catalysts, J. Catal. 174 (1998) 246–249, http://dx.doi.org/10.1006/jcat.1998.1966.

2018-2

ORIGINALITY REPORT

17%	6%	17%	0%
SIMILARITY INDEX	INTERNET SOURCES	PUBLICATIONS	STUDENT PAPERS

PRIMARY SOURCES

1	docplayer.net Internet Source	4%
2	Rodiansono Rodiansono, Maria Dewi Astuti, Kamilia Mustikasari, Sadang Husain, Sutomo Sutomo. "Recent progress in the direct synthesis of y-valerolactone from biomass-derived sugars catalysed by Raney nickel-tin alloy supported on aluminium hydroxide", Catalysis Science & Technology, 2020 Publication	4%
3	A P Damayanti, H P Dewi, Ibrahim, Rodiansono. "Selective hydrogenation of levulinic acid to y-valerolactone using bimetallic Pd-Fe catalyst supported on titanium oxide", IOP Conference Series: Materials Science and Engineering, 2021 Publication	3%
4	Rodiansono Rodiansono, Maria Dewi Astuti, Takayoshi Hara, Nobuyuki Ichikuni, Shogo Shimazu. " One-pot selective conversion of C5-furan into 1,4-pentanediol over bulk Ni–Sn	3%

alloy catalysts in an ethanol/H O solvent mixture ", Green Chemistry, 2019
Publication

5 Changming Li, Yudi Chen, Shitong Zhang, Simin Xu, Junyao Zhou, Fei Wang, Min Wei, David G. Evans, Xue Duan. "Ni–In Intermetallic Nanocrystals as Efficient Catalysts toward Unsaturated Aldehydes Hydrogenation", Chemistry of Materials, 2013 2%
Publication

6 "Graphical abstract TOC", Molecular Catalysis, 2018 2%
Publication

Exclude quotes	On	Exclude matches	< 2%
Exclude bibliography	On		